

## **Supporting Information**

### **Nature of active nickel sites and initiation mechanism for ethylene oligomerization on heterogeneous Ni-beta catalysts**

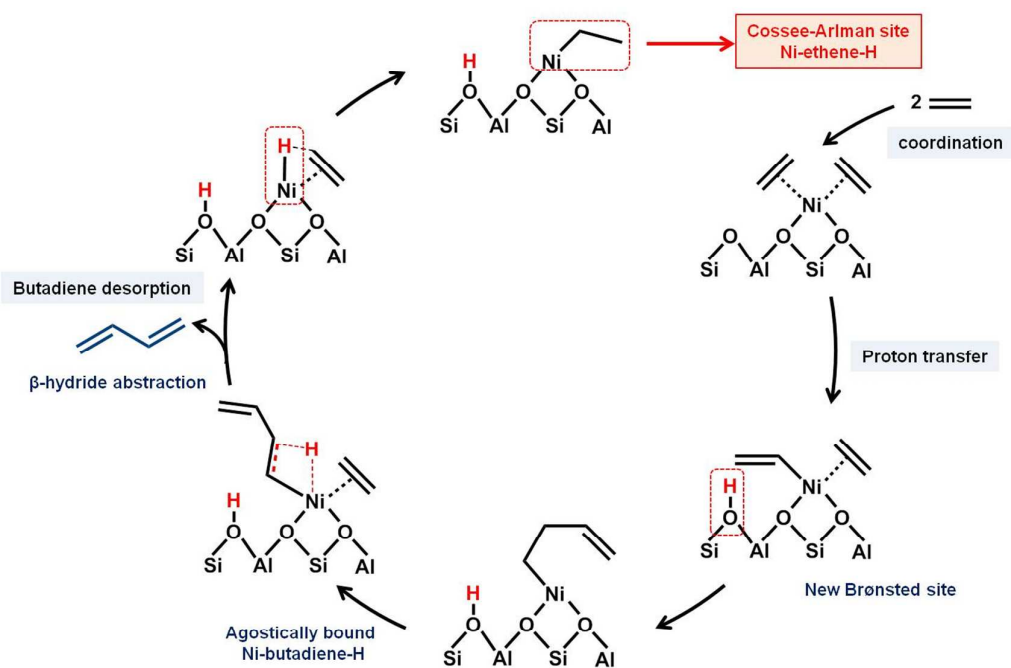
Sara Moussa, Patricia Concepción, María A. Arribas, and Agustín Martínez\*

Instituto de Tecnología Química, Universitat Politècnica de València – Consejo Superior de Investigaciones Científicas (UPV-CSIC), Avda. de los Naranjos s/n, 46022 Valencia, Spain

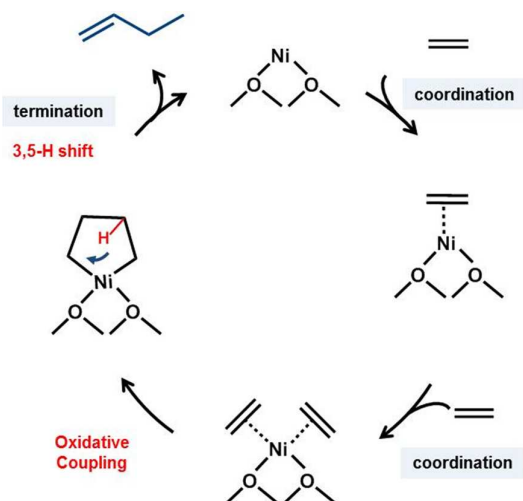
\* Corresponding author: Prof. A. Martínez

E-mail address: [amart@itq.upv.es](mailto:amart@itq.upv.es)

**Scheme S1.** Simplified route proposed for the generation of Cossee-Arlman centers (Ni-H or Ni-ethene-H) in nickel-aluminosilicate catalysts initiated by proton transfer<sup>1</sup>. According to this pathway, the heterolytic cleavage of a C-H bond of ethylene coordinated at a charge-balancing Ni<sup>2+</sup> site leads to a nickel-vinyl species and H that generates a new Brønsted acid site on a nearby lattice O atom. Insertion of a second ethylene molecule into the Ni-C bond of the Ni-vinyl species forms Ni-butenyl which releases butadiene through  $\beta$ -hydride abstraction to the same Ni ion, creating the Ni-H Cossee-Arlman site<sup>1</sup>.



**Scheme S2.** Metallacycle mechanism proposed for the oligomerization of ethylene catalyzed by nickel.



The metallacycle route, originally proposed for the selective trimerization of ethylene on Phillips ( $\text{Cr}/\text{SiO}_2$ ) catalysts<sup>2-5</sup>, involves the formation of a metallacyclopentane intermediate via oxidative coupling of two ethylene molecules coordinated to the metal site. Chain propagation then occurs by insertion of additional ethylene molecules into any of the two metal-C bonds forming larger metallacycles, while chain termination can take place through a direct hydrogen shift or via stepwise  $\beta$ -hydride elimination to the metal site followed by reductive elimination releasing the corresponding linear  $\alpha$ -olefin. More recently, the metallacycle mechanism has been suggested in order to account for the product distribution during the heterogeneous oligomerization of ethylene over Ni-Al-SBA-15 catalysts<sup>6</sup>.

**Table S1.** Characteristic mass fragmentations ( $m/z$  signals) and relative peak intensities, taking the most intense  $m/z$  peak for each compound as 100, for ethylene and relevant reaction products. The specific  $m/z$  values used in the identification of each compound during the acquisition of the online MS spectra are highlighted in bold.

	$m/z$ values										
	26	27	28	29	30	43	55	56	58	69	84
Ethylene	<b>55</b>	62	100	5	-	-	-	-	-	-	-
Ethane	22	35	100	21	<b>30</b>	-	-	-	-	-	-
Butenes	10	25	30	15	1	6	50	<b>100</b>	5	-	-
Butane	10	40	35	45	3	100	2	1	<b>15</b>	-	-
Hexenes	5	35	5	20	3	60	65	100	10	25	<b>30</b>

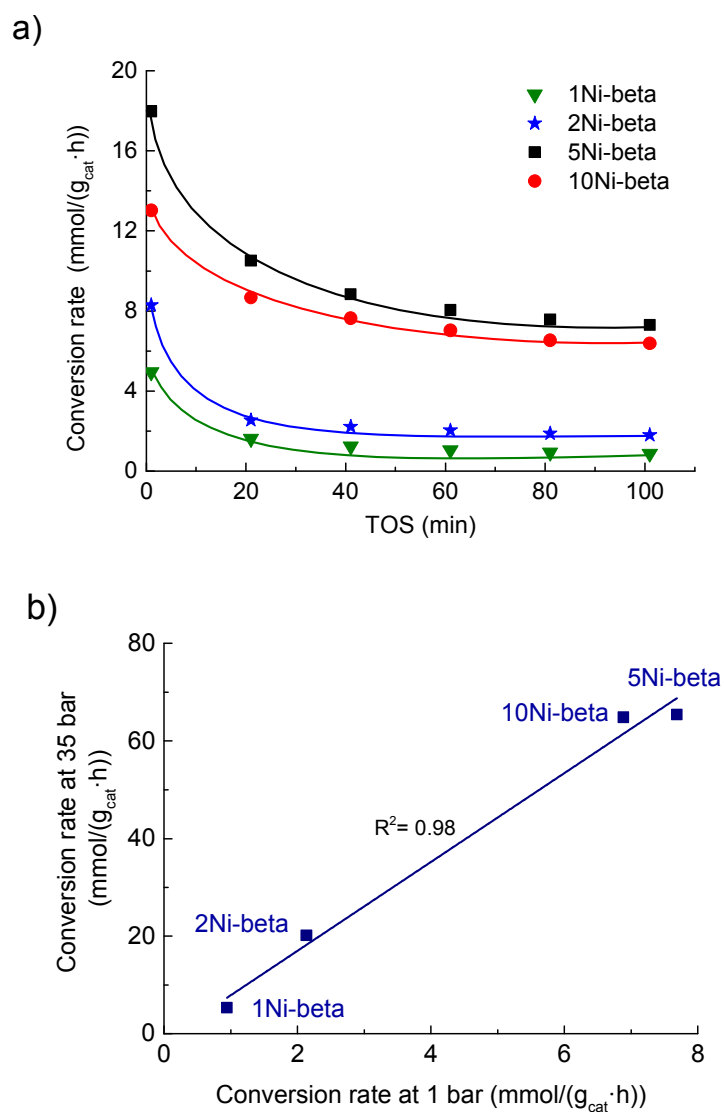


**Figure S1.** a) Ethylene conversion rates at 120 °C, 1 bar, and WHSV of 33 h<sup>-1</sup> as a function of time-on-stream (TOS) for Ni-beta catalysts loaded with different amounts of nickel (1-10 wt%); b) Correlation between the steady state ethylene conversion rates at the reaction pressure of 1 bar (120 °C, 33 h<sup>-1</sup>) and 35 bar (120 °C, 2.1 h<sup>-1</sup>).

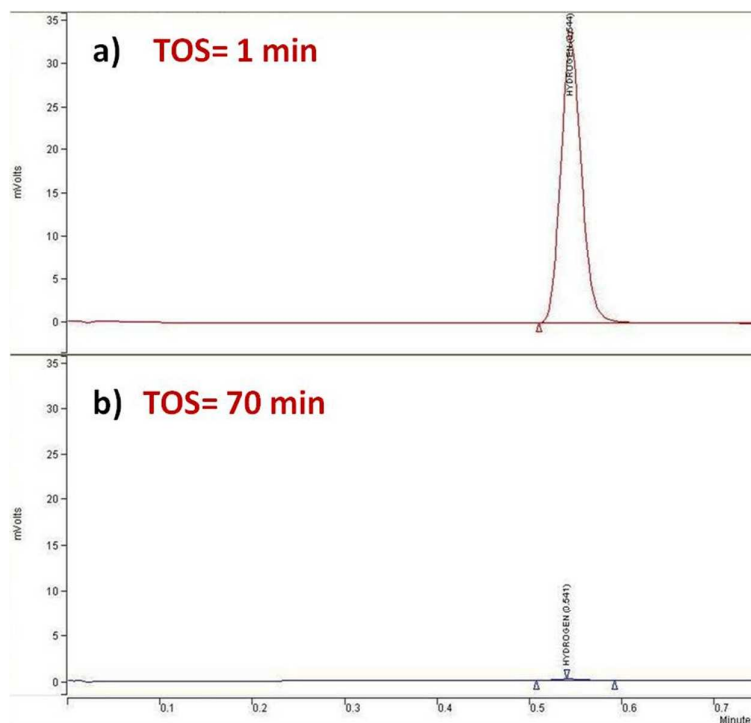


**Figure S2.** Chromatograms evidencing the initial formation of  $H_2$  upon reacting 5Ni-beta with ethylene at 120 °C and 1 bar for 1 min (a) and its practical absence after 70 min of reaction (b). The analyses were performed by manually injecting a representative sample of the gaseous effluent in a Varian 3800 GC specially equipped for  $H_2$  detection (5Å Molecular Sieve column, TCD-type detector, Ar as carrier gas).

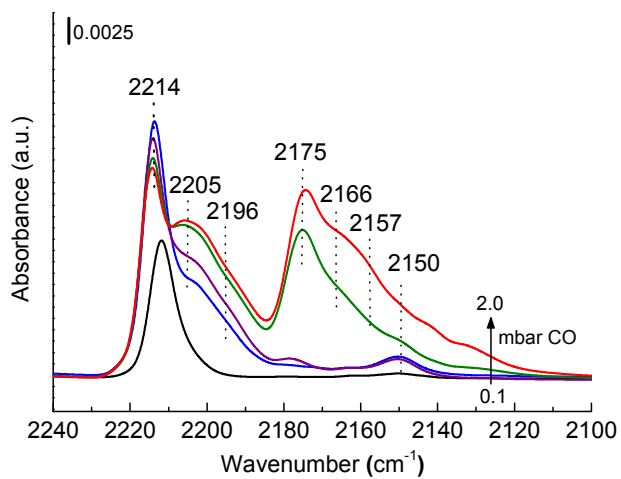


**Figure S3.** FTIR spectra of CO adsorption recorded at -176 °C for pre-reacted (i.e. after in situ pretreatment in flowing N<sub>2</sub> at 300 °C) 5Ni-beta sample at increasing CO pressures (0.1→2.0 mbar).

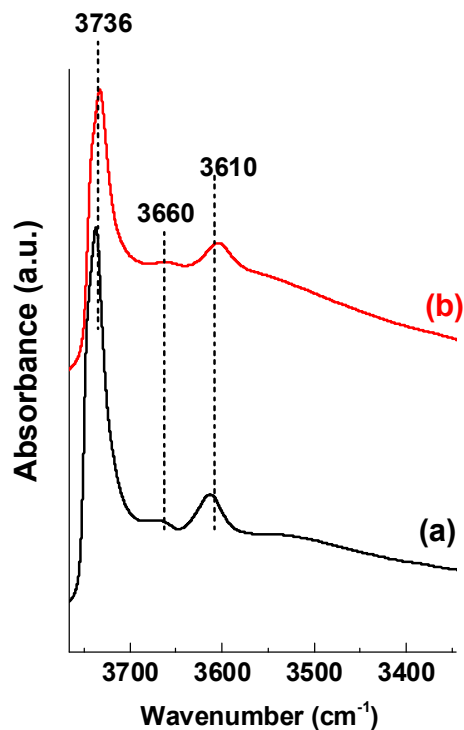


**Figure S4.** Normalized FTIR spectra in the OH stretching region of a) pristine H-beta zeolite, and b) 5Ni-beta sample after *in situ* pretreatment in flowing N<sub>2</sub> at 300 °C.

The FTIR spectrum of activated pristine H-beta zeolite in the OH stretching region (spectrum a) showed three distinct features with maxima at ca. 3736, 3660, and 3610 cm<sup>-1</sup> assigned to the  $\nu(\text{O-H})$  vibration modes of silanols, extraframework aluminium species, and Brønsted acid sites, respectively. After nickel incorporation (spectrum b), a reduction in the intensities of the peaks at 3736 and 3610 cm<sup>-1</sup> is observed due to the replacement of some acidic protons by nickel ions. Furthermore, no additional peak in the 3630–3650 cm<sup>-1</sup> region attributable to Ni-OH species<sup>7</sup> could be detected in the activated 5Ni-Beta sample.



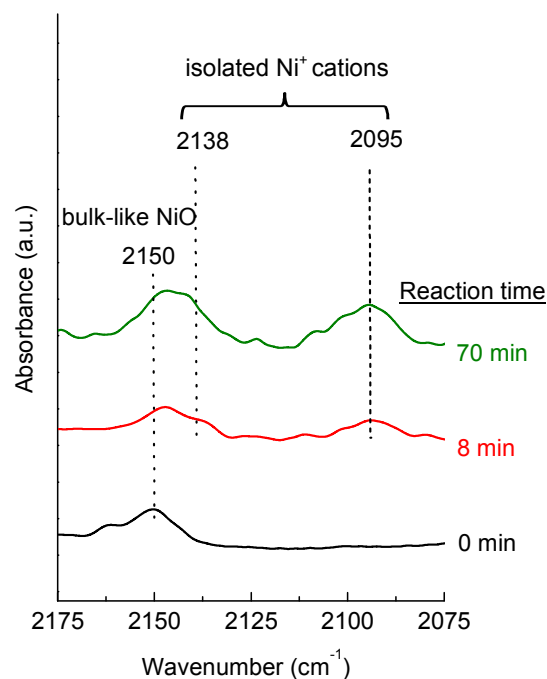


**Figure S5.** Low temperature FTIR-CO spectra at low CO coverage (0.1 mbar) for the 5Ni-beta catalyst showing the development of dicarbonyl  $\text{Ni}^+$  bands at 2138 and 2095  $\text{cm}^{-1}$  upon reaction with ethylene at 120 °C and 1 bar for selected reaction times. The component at 2150  $\text{cm}^{-1}$  of CO coordinated to unsaturated  $\text{Ni}^{2+}$  species on the surface of bulk-like NiO particles (reported as inactive in ethylene oligomerization) remains almost unaffected during the catalytic reaction. Spectra are up-shifted for better visualization.

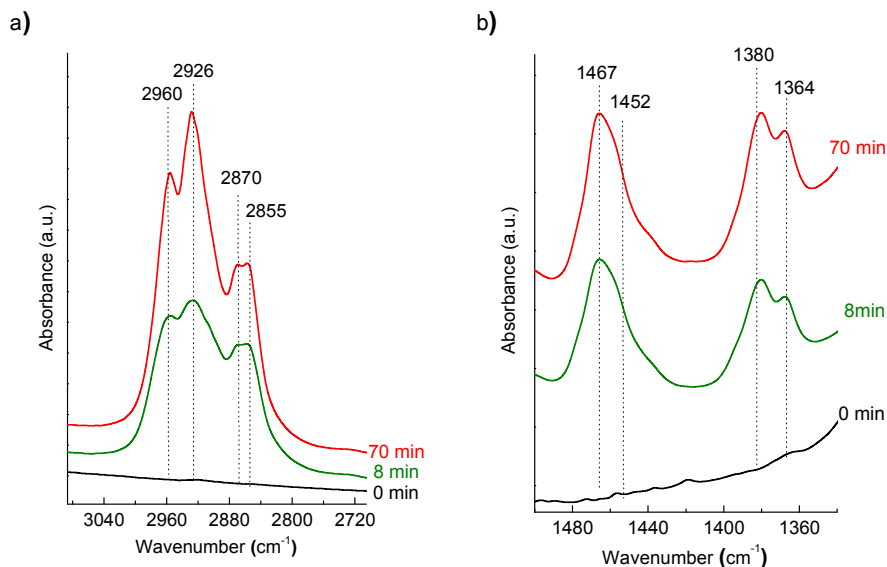


**Figure S6.** FTIR spectra (normalized by overtone area) in the C-H stretching (a) and bending (b) vibration regions for 5Ni-beta in its pre-reacted state (spectrum at 0 min) and after reaction with ethylene at 120 °C and 1 bar for 8 and 70 min and subsequent evacuation of the cell at 120 °C for 1 h under dynamic vacuum of  $10^{-5}$  mbar. The characteristic  $sp^3$  C-H stretching and bending IR bands of  $CH_3$  ( $\nu_{as}= 2960\text{ cm}^{-1}$ ,  $\nu_s= 2870\text{ cm}^{-1}$ ,  $\delta_s= 1364\text{-}1380\text{ cm}^{-1}$ ,  $\delta_{as}= 1440\text{-}1470\text{ cm}^{-1}$ ) and  $CH_2$  ( $\nu_{as}= 2926\text{ cm}^{-1}$ ,  $\nu_s= 2855\text{ cm}^{-1}$ ,  $\delta= 1440\text{-}1470\text{ cm}^{-1}$ ) groups<sup>8-11</sup> are clearly perceived.

From the intensities of the peaks assigned to  $CH_2$  and  $CH_3$  asymmetric stretches, a  $CH_2/CH_3$  ratio of ca. 1.14 and 1.24 is obtained for the irreversibly adsorbed hydrocarbons (spectators) after 8 and 70 min of reaction, respectively, evidencing a minor increase in chain length with reaction time. Considering that a  $CH_2/CH_3$  ratio of 2 and 3 has been reported for the asymmetric C-H stretches of *n*-hexane and *n*-octane, respectively<sup>12</sup>, we infer that those spectators are mainly short-chain aliphatic acyclic hydrocarbons.

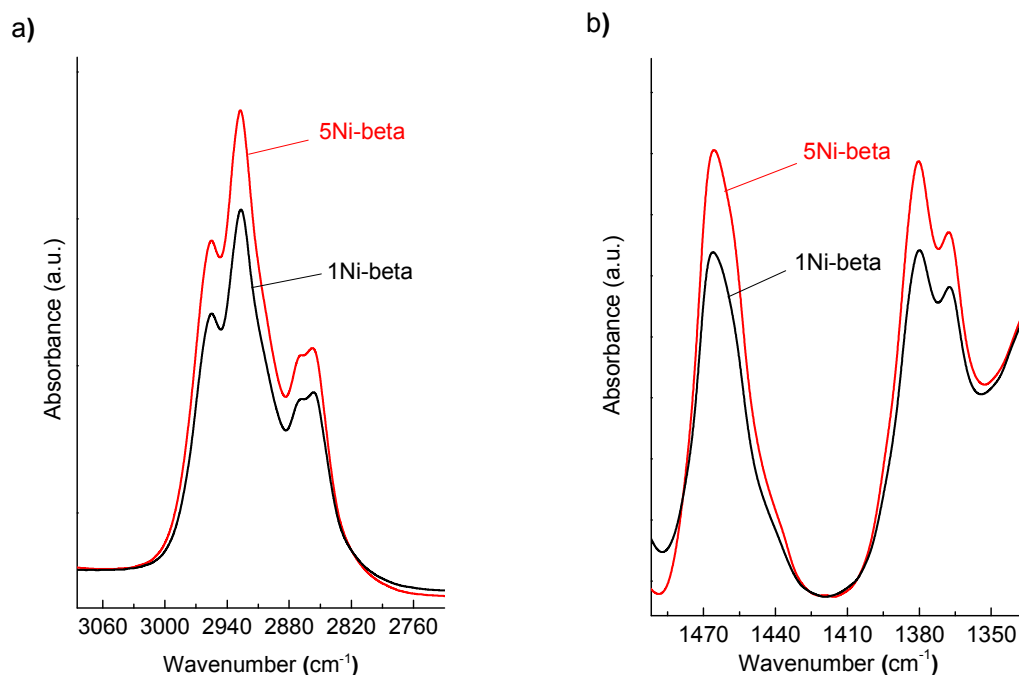


**Figure S7.** Normalized FTIR spectra in the C-H stretching (a) and bending (b) vibration regions for Ni-beta samples loaded with 1 and 5 wt% Ni after in situ reaction with ethylene for 70 min at 120 °C and 1 bar followed by evacuation at this temperature for 1 h under dynamic vacuum of  $10^{-5}$  mbar. The higher concentration of hydrocarbon species irreversibly adsorbed on the surface of the highly-loaded 5Ni-beta catalyst exhibiting a 2.5-fold lower amount of Brønsted acid sites than 1Ni-beta<sup>13</sup> is an indication that they predominantly form at the cationic nickel centers.

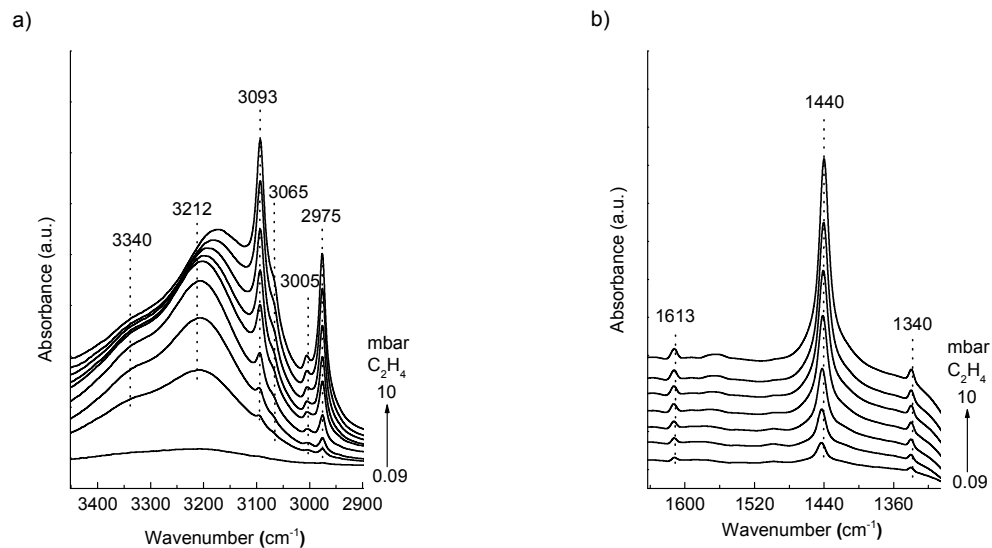


**Figure S8.** FTIR spectra in the C-H stretching (a) and bending (b) regions of ethylene adsorbed at  $-100\text{ }^{\circ}\text{C}$  on pristine H-beta zeolite at increasing ethylene doses (from 0.09 to 10 mbar). Spectra have been up-shifted for clarity.

Ethylene adsorbs only physically on the surface OH groups of Ni-free H-beta zeolite, as inferred from the presence of IR bands of  $\text{CH}_2$  groups in the C-H stretching (3093, 3065, 3005, and  $2975\text{ cm}^{-1}$ , left graph) and bending ( $1440$  and  $1340\text{ cm}^{-1}$ ) regions and the  $\nu[\text{C}=\text{C}]$  stretching band at  $1613\text{ cm}^{-1}$ . Broad IR bands peaking at around  $3340$  and  $3210\text{ cm}^{-1}$  correspond to the shift towards lower frequencies of the O-H stretching bands of the zeolite perturbed by ethylene.

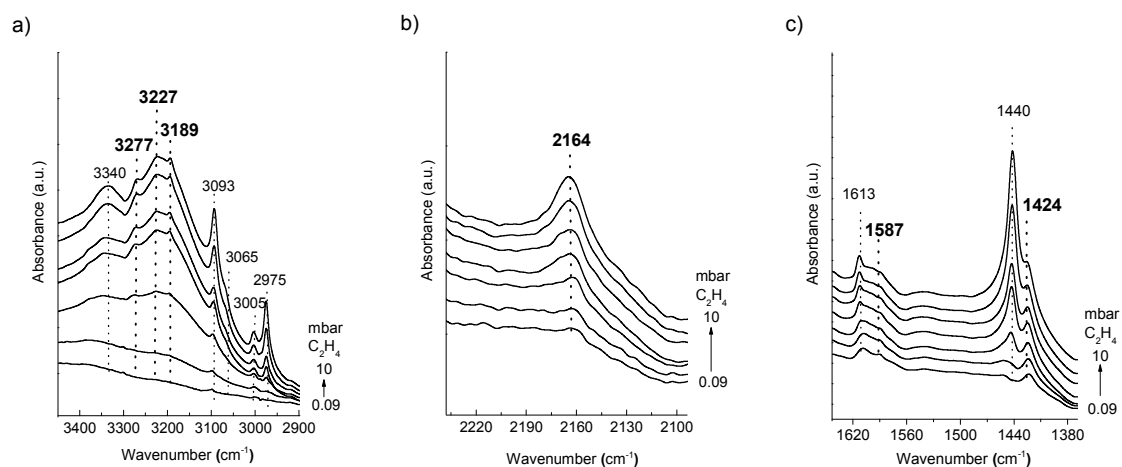


**Figure S9.** FTIR spectra recorded in different IR regions (a-c) upon adsorption of ethylene at -100 °C on 5Ni-beta catalyst at increasing ethylene doses from 0.09 to 10 mbar. Spectra have been up-shifted for clarity. The bands related to ethylene  $\pi$ -bonded to  $\text{Ni}^{2+}$  cations and acetylenic species (see main text) are highlighted in bold.

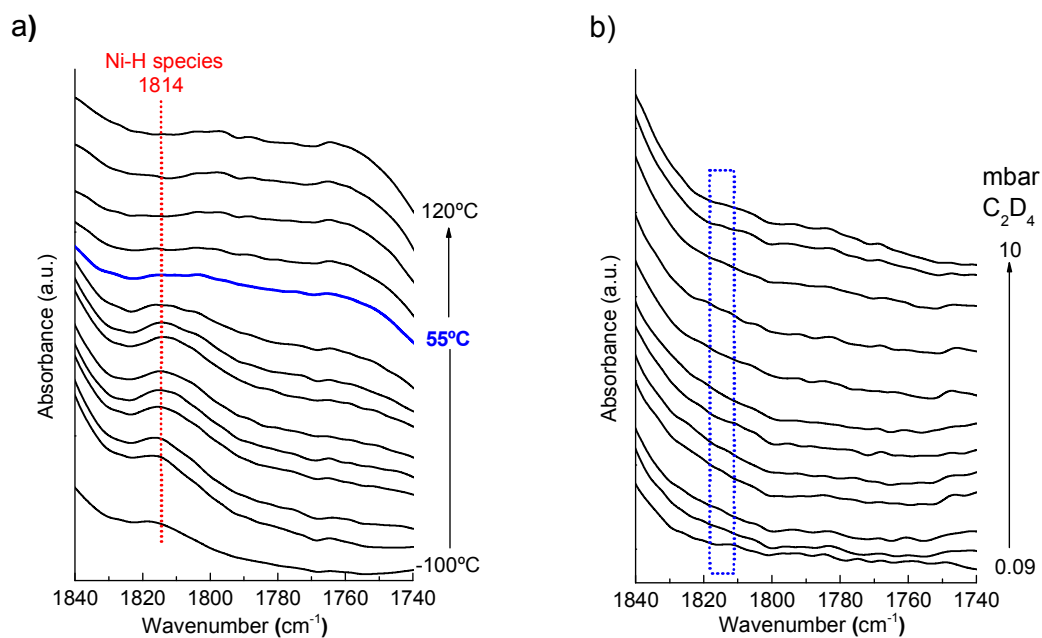


**Figure S10.** FTIR spectra acquired in the Ni-H region for 5Ni-beta upon adsorption of ethylene from -100 °C to 120 °C (a) and of deuterated ethylene at -100 °C and increasing coverage from 0.09 to 10 mbar (b). Spectra have been up-shifted for clarity.

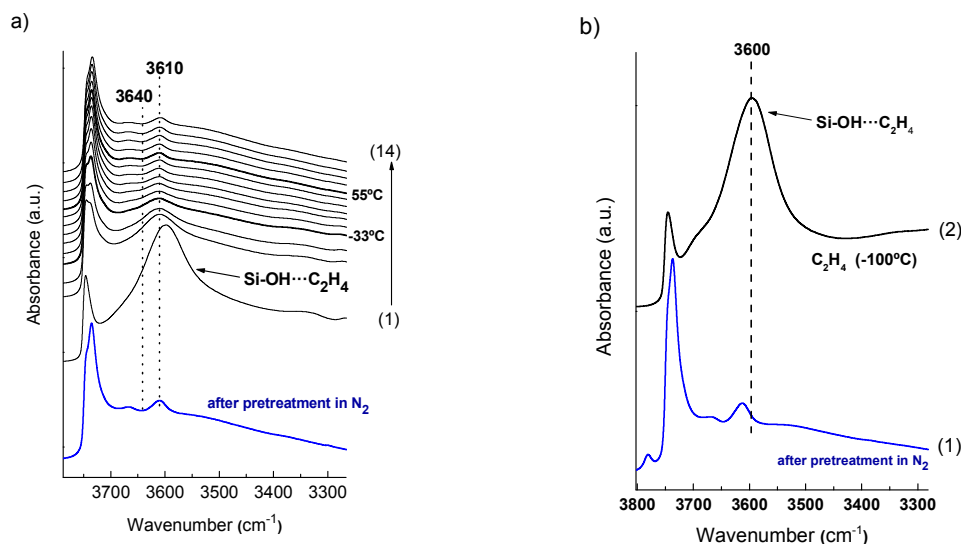


**Figure S11.** a) Temperature-resolved FTIR spectra for 5Ni-beta in the OH stretching region after in situ pretreatment in flowing N<sub>2</sub> at 300°C (blue bold line) and during in situ reaction of ethylene (black lines) at a constant pressure of 1.5 mbar in the temperature range of : (1) -100°C, (2) -58°C, (3) 48°C, (4) -33°C, (5) -25°C, (6) -15°C, (7) -4°C, (8) 5°C, (9) 26°C, (10) 55°C, (11) 66°C, (12) 88°C, (13) 107°C, (14) 120°C. Spectra have been up-shifted for the sake of clarity; b) FTIR spectra in the OH stretching region of pristine H-beta zeolite after in situ pretreatment in flowing N<sub>2</sub> at 300°C (1), and upon ethylene adsorption (10 mbar) at -100 °C (2).

As seen in Figure S11a, when ethylene is contacted with 5Ni-Beta catalyst at -100°C, it physisorbs on the catalyst surface resulting in a pronounced decrease of the silanol band at ca. 3736 cm<sup>-1</sup> that shifts to lower frequencies producing an intense broad band with maxima at ca. 3605 cm<sup>-1</sup>.<sup>10</sup> Indeed, the perturbed OH band (Si-OH...C<sub>2</sub>H<sub>4</sub> molecular complex) is also detected when ethylene was adsorbed over pristine H-beta zeolite at -100°C (Figure S11b). As observed in Figure S11a, the IR spectra in the OH region is dominated from -100 °C to -33 °C by the broad perturbed OH band vibrating in the region where the formation of new OH groups would be observed (ca. 3610 and 3640 cm<sup>-1</sup>)<sup>14,15</sup>. This makes an unequivocal conclusion on the possible formation of new OH groups in this temperature range unfeasible. However, at temperatures above ca. -33°C (at which vinyl intermediates start to be detected),

where the perturbed OH band at  $3605\text{ cm}^{-1}$  does no longer disturb the peaks in this region, there are no spectroscopic signs evidencing the formation of new OH groups.



## References

1. Brogaard, R. Y.; Olsbye, U. Ethene Oligomerization in Ni-Containing Zeolites: Theoretical Discrimination of Reaction Mechanisms. *ACS Catal.* **2016**, *6*, 1205-1214.
2. McGuinness, D. S. Olefin Oligomerization via Metallacycles: Dimerization, Trimerization, Tetramerization, and Beyond. *Chem. Rev.* **2011**, *111*, 2321-2341.
3. Briggs, J. R. Selective trimerization of ethylene to hex-1-ene. *J. Chem. Soc., Chem. Commun.* **1989**, 674-675.
4. Nenu, C. N.; Weckhuysen, B. M. Single-site heterogeneous Cr-based catalyst for the selective trimerization of ethylene. *Chem. Commun.* **2005**, 1865-1867.
5. Ruddick, V. J.; Badyal, J. P. S. Early stages of ethylene polymerization using the Phillips CrO<sub>x</sub>/silica catalyst. *J. Phys. Chem. B* **1998**, *102*, 2991-2994.
6. Andrei, R. D.; Popa, M. I.; Fajula, F.; Hulea, V. Heterogeneous oligomerization of ethylene over highly active and stable Ni-AISBA-15 mesoporous catalysts. *J. Catal.* **2015**, *323*, 76-84.
7. Hall, D. S.; Lockwood, D. J.; Poirier, S.; Bock, C.; MacDougall, B. R. Raman and Infrared Spectroscopy of  $\alpha$  and  $\beta$  Phases of Thin Nickel Hydroxide Films Electrochemically Formed on Nickel. *J. Phys. Chem. A* **2012**, *116*, 6771-6784.
8. Tanaka, M.; Itadani, A.; Kuroda, Y.; Iwamoto, M. Effect of Pore Size and Nickel Content of Ni-MCM-41 on Catalytic Activity for Ethene Dimerization and Local Structures of Nickel Ions. *J. Phys. Chem. C* **2012**, *116*, 5664-5672.
9. Groppo, E.; Lamberti, C.; Bordiga, S.; Spoto, G.; Zecchina, A. The Structure of Active Centers and the Ethylene Polymerization Mechanism on the Cr/SiO<sub>2</sub> Catalyst: A Frontier for the Characterization Methods. *Chem. Rev.* **2005**, *105*, 115-183.
10. Groppo, E.; Lamberti, C.; Bordiga, S.; Spoto, G.; Damin, A.; Zecchina, A. FTIR Investigation of the H<sub>2</sub>, N<sub>2</sub>, and C<sub>2</sub>H<sub>4</sub> Molecular Complexes Formed on the Cr(II) Sites in the Phillips Catalyst: a Preliminary Step in the understanding of a Complex System. *J. Phys. Chem. B* **2005**, *109*, 15024-15031.
11. Groppo, E.; Lamberti, C.; Bordiga, S.; Spoto, G.; Zecchina, A. In situ FTIR spectroscopy of key intermediates in the first stages of ethylene polymerization on the Cr/SiO<sub>2</sub> Phillips catalyst: Solving the puzzle of the initiation mechanism?. *J. Catal.* **2006**, *240*, 172-181.
12. Smith, B.C. How to Properly Compare Spectra, and Determining Alkane Chain Length from Infrared Spectra. *Spectroscopy* **2015**, *30*, 40-46.
13. Martinez, A.; Arribas, M. A.; Concepcion, P.; Moussa, S. New bifunctional Ni-H-Beta catalysts for the heterogeneous oligomerization of ethylene. *Appl. Catal., A* **2013**, *467*, 509-518.
14. Delley, M. F.; Núñez-Zarur, F.; Conley, M. P.; Comas-Vives, A.; Siddiqi, G.; Norsic, S.; Monteil, V.; Safonova, O. V.; Copéret, C. Proton transfers are key elementary steps in ethylene polymerization on isolated chromium(III) silicates. *PNAS* **2014**, *111*, 11624-11629.
15. Conley, M. P.; Delley, M. F.; Siddiqi, G.; Lapadula, G.; Norsic, S.; Monteil, V.; Safonova, O. V.; Copéret, C. Polymerization of ethylene by silica-supported dinuclear Cr(III) sites through an initiation step involving C-H bond activation. *Angew. Chem. Int. Ed.* **2014**, *53*, 1872-1876.